SIAM J. Applied Dynamical Systems
Vol. 7, No. 2, pp. 249–264

Surface Gap Solitons at a Nonlinearity Interface*

Tomáš Dohnal† and Dmitry Pelinovsky‡

Abstract. We demonstrate existence of waves localized at the interface of two nonlinear periodic media with different coefficients of the cubic nonlinearity via the one-dimensional Gross–Pitaevsky equation. We call these waves the surface gap solitons (SGSs). In the case of smooth symmetric periodic potentials, we study analytically bifurcations of SGSs from standard gap solitons and determine numerically the maximal jump of the nonlinearity coefficient allowing for SGS existence. We show that the maximal jump vanishes near the thresholds of bifurcations of gap solitons. In the case of continuous potentials with a jump in the first derivative at the interface, we develop a homotopy method of continuation of SGS families from the solution obtained via gluing of parts of the standard gap solitons and study existence of SGSs in the photonic band gaps. We explain the termination of the SGS families in the interior points of the band gaps from the bifurcation of linear bound states in continuous nonsmooth potentials.

Key words. surface gap solitons, Gross–Pitaevsky equation, nonlinear Schrödinger equation, nonlinearity interface

AMS subject classifications. 35Q60, 37J45, 78A40

DOI. 10.1137/060676751

1. Introduction.

We are concerned with localized waves at the interface of two periodic nonlinear media called surface gap solitons (SGSs). One of the first publications on optical solitons propagating along material interfaces is [17], where the interface of a linear and a focusing Kerr nonlinear medium is studied. In the last two years relevant publications in the context of nonlinear optics have dealt, for instance, with discrete surface solitons in nonlinear waveguide arrays [4, 10, 16], SGSs at the interface of a uniform and a periodic medium with the defocusing cubic nonlinearity [7], and surface vortex solitons at the interface of two periodic media with different mean values of the refractive index and with saturable nonlinearity [5, 6]. One of the typical models employed in the theory of gap solitons is the one-dimensional nonlinear Schrödinger (NLS) equation with cubic nonlinearity and periodic potential called the Gross–Pitaevsky equation.

We investigate here the existence of surface waves at the interface of two media with identical periodic linear parts of the refractive index and with different cubic nonlinearities. It is known that for most photonic materials a variation in the nonlinear part of the refractive index n_2 is necessarily accompanied by a larger change in the linear part n_0. Nevertheless,

*Received by the editors December 5, 2006; accepted for publication (in revised form) by B. Sandstede September 5, 2007; published electronically April 23, 2008.
http://www.siam.org/journals/siads/7-2/67675.html
†Seminar for Applied Mathematics, ETH Zürich, Zürich, Switzerland (dohnal@math.ethz.ch). This author is supported by an ETH Research Fellowship.
‡Department of Mathematics, McMaster University, Hamilton, Ontario, Canada, L8S 4K1 (dmpeli@math.mcmaster.ca). This author is supported by the Humboldt Research Fellowship hosted at Institut für Analysis, Dynamik und Modellierung, Fakultaet für Mathematik und Physik at Universität Stuttgart.

certain materials exhibit large variations in n_2 accompanied by small variations in n_0; see [1, 15]. Localized states have been studied theoretically in media with constant n_0 and spatially periodic n_2 in [3].

Each of the two periodic nonlinear media supports at least two families of standard gap solitons in every bounded nonempty frequency gap. One family is always unstable, while the other can be stable depending on the locations of spectral bands and bifurcations of eigenvalues from the band edges [13]. The potentially stable family looks like a single-humped envelope soliton with exponential decay and oscillations near the central peak. Multihumped envelope solitons may also exist in such periodic nonlinear media, but we shall focus herein on existence of a single-humped solution localized near the interface between the two periodic nonlinear media.

The paper is organized as follows. Section 2 reviews Floquet theory for the governing Gross–Pitaevsky equation and summarizes the results on existence of gap solitons. In section 3 we study the existence of SGSs for a smooth symmetric periodic potential function and find the maximal allowed jump in the nonlinearity coefficient between the two media for existence of SGSs. Section 4 discusses bifurcations and existence of SGSs for a continuous potential function with a derivative jump at the nonlinearity interface. Section 5 concludes the paper with conjectures on the stability of SGSs.

2. Background: Floquet theory and gap soliton existence. We consider the one-dimensional periodic cubic Schrödinger equation in the form

$$iu_t = -u_{xx} + V(x)u - \Gamma(x)|u|^2 u, \quad x \in \mathbb{R}, \quad t \geq 0, \tag{2.1}$$

where x and t are the spatial and temporal variables, respectively, $V(x)$ is a real, continuous, and d-periodic potential, and $\Gamma(x) = \Gamma_\pm$ for $\pm x > 0$ is a real nonlinearity coefficient with constants Γ_+ and Γ_-. The positive values of $\Gamma(x)$ correspond to the focusing nonlinearity and the negative values of $\Gamma(x)$ to the defocusing nonlinearity.

We are interested in the existence of stationary solutions of (2.1) localized near the interface at $x = 0$ and having the form

$$u(x,t) = e^{-i\omega t}\phi(x) \quad \text{s.t.} \quad \phi : \mathbb{R} \to \mathbb{R}, \quad \phi \to 0 \ \text{ as } \ |x| \to \infty. \tag{2.2}$$

The function $\phi(x)$ has to satisfy the second-order nonautonomous ODE

$$-\phi'' - \omega\phi + V(x)\phi - \Gamma(x)\phi^3 = 0, \tag{2.3}$$

which can be cast in the Hamiltonian form with the Hamiltonian function

$$H[\phi] = \frac{1}{2}\left[(\phi')^2 + \omega\phi^2 - V(x)\phi^2\right] + \frac{1}{4}\Gamma(x)\phi^4. \tag{2.4}$$

Since $\Gamma(x)$ is discontinuous at $x = 0$, $\phi(x)$ is a weak solution of the ODE (2.3) in $\phi \in C^2(\mathbb{R}_+ \cup \mathbb{R}_-)$, such that the second derivative $\phi''(x)$ may have a jump at $x = 0$. The continuously differentiable solution $\phi \in C^1(\mathbb{R})$ is a critical point of the energy functional

$$E_\omega[\phi] = \frac{1}{2}\int_{\mathbb{R}} \left[|\phi'|^2 + \omega|\phi|^2 - V(x)|\phi|^2\right] dx + \frac{1}{4}\int_{\mathbb{R}} \Gamma(x)|\phi|^4 dx,$$

such that the first variation $E'_\omega[\phi]$ recovers the ODE (2.3).

Replacing t by z in (2.1) and (2.2), the x-localized solution $u(x,z)$ can be viewed as a spatial soliton propagating along the direction z and localized in the transverse direction x. The parameter ω plays the role of the propagation constant. Other applications of the ODE (2.3) occur in the theory of stationary solutions of the nonlinear Maxwell and Klein–Gordon equations in one dimension.

As we show below, the localized solutions of the ODE (2.3) decay exponentially as $|x| \to \infty$ only if ω belongs to the frequency gaps in the continuous spectra of the operator $L := -\partial_{xx} + V(x)$ called the photonic band gaps. To do so, we recall the basic Floquet theory (see [2, 9]) for the Hill equation

$$L\psi(x) = -\psi''(x) + V(x)\psi(x) = \omega\psi(x), \qquad x \in \mathbb{R}. \tag{2.5}$$

The bounded solutions $\psi(x)$ of the Hill equation (2.5) are usually called Bloch functions. Given a real, continuous, and d-periodic potential $V(x)$, bounded solutions $\psi(x)$ exist for ω in a union of (possibly disjoint) spectral bands

$$\Sigma := [\omega_0, \omega_1] \cup [\omega_2, \omega_3] \cup [\omega_4, \omega_5] \cup \dots,$$

where $\omega_{2n-2} < \omega_{2n-1} \leq \omega_{2n}$, $n \in \mathbb{N}$, and $\omega_n \to \infty$ as $n \to \infty$. The set Σ represents the complete (purely continuous) spectrum of the operator L [2]. We shall *assume* for simplicity that all spectral bands are disjoint with $\omega_{2n-1} < \omega_{2n}$, $n \in \mathbb{N}$, such that all finite frequency gaps are nonempty.

For a fixed ω in the interior point of Σ, both fundamental solutions of the second-order ODE (2.5) are quasi-periodic in x and have the representation $\psi = p_\pm(x)e^{\pm ikx}$, where $p_\pm(x) = p_\pm(x+d)$ and $k \in \left[0, \frac{\pi}{d}\right]$. The parameter k parameterizes the frequency parameter ω, such that we shall use the notation $\omega = \omega_{2n,2n+1}(k)$ for the spectral band in $\omega \in [\omega_{2n}, \omega_{2n+1}]$. If the nth band is separated from the $(n+1)$th band (i.e., $\omega_{2n-1} < \omega_{2n}$ and $\omega_{2n+1} < \omega_{2n+2}$), then $\omega'_{2n,2n+1}(k) = 0$ and $\omega''_{2n,2n+1}(k) \neq 0$ at the endpoints $k = 0$ and $k = \frac{\pi}{d}$ [8].

When $\omega = \omega_n$, one of the solutions $\psi = \psi_n(x)$ is either d-periodic (corresponding to $k = 0$) or d-antiperiodic (corresponding to $k = \frac{\pi}{d}$), and the other fundamental solution $\psi(x)$ grows linearly in x. For a fixed $\omega \in \mathbb{R} \setminus \Sigma$ the two fundamental solutions of (2.5) grow exponentially in either x or $-x$ and have the representation $\psi = u_\pm(x)e^{\pm\kappa x}$, where $u_\pm(x)$ is either periodic or antiperiodic and $\kappa = \kappa(\omega) \in \mathbb{R}_+$. The functions $u_\pm(x)$ are periodic (antiperiodic) if the bounded solutions $\psi_n(x)$ are periodic (antiperiodic) at the band edges ω_{2n-1} and ω_{2n}, which surround the band gap.

Suppose that $\phi(x)$ is a localized solution of the ODE (2.3). It is then obvious from the linearized analysis that the solution $\phi(x)$ decays exponentially as $|x| \to \infty$ only if $\omega \in \mathbb{R} \setminus \Sigma$. It was shown under fairly general assumptions (see [13] and references therein) that the families of gap solitons of the ODE (2.3) with constant coefficient $\Gamma(x) = \Gamma_0$ undertake a local bifurcation from all points $\omega = \omega_{2m}$, $m \geq 0$, to the left if $\Gamma_0 > 0$ and from all points $\omega = \omega_{2m+1}$, $m \geq 0$, to the right if $\Gamma_0 < 0$ (the term *local bifurcation* means that $\|\phi\|_{L^\infty} \to 0$ as $\omega \to \omega_n$). This conjecture was rigorously proved in [11], where existence of exponentially decaying gap solitons in $H^1(\mathbb{R})$ was confirmed in every finite frequency gap $\omega \in (\omega_{2m-1}, \omega_{2m})$, $m \in \mathbb{N}$, and in the semi-infinite frequency gap $\omega < \omega_0$ for $\Gamma_0 > 0$. We use this result but

simplify our consideration by working with the class of symmetric potentials $V = V_0(x)$, where $V_0(-x) = V_0(x)$ on $x \in \mathbb{R}$. In particular, we shall perform numerical computations with

$$V_0(x) = \sin^2\left(\frac{\pi x}{d}\right), \quad d = 10, \tag{2.6}$$

which has a minimum at $x = 0$, i.e., at our interface location. The spectral bands and gaps of $V_0(x)$ are approximated numerically from the Hill equation (2.5). For instance, the first five band edges of the potential (2.6) are located as follows:

$$\omega_0 \approx 0.283, \quad \omega_1 \approx 0.291, \quad \omega_2 \approx 0.747, \quad \omega_3 \approx 0.843, \quad \omega_4 \approx 1.057.$$

As seen in Figure 1 of [13], the Bloch functions $\psi = \psi_n(x)$ at the band edges $\omega = \omega_n$, $n \geq 0$, have the following symmetry properties:

$$\begin{aligned} &\psi_n(-x) = \psi_n(x), \ n \in \{0, 1, 4, 5, 8, 9, \ldots\}, \\ &\psi_n(-x) = -\psi_n(x), \ n \in \{2, 3, 6, 7, \ldots\}. \end{aligned} \tag{2.7}$$

Symmetry properties (2.7) can be proved for any even potential $V_0(-x) = V_0(x)$. Indeed, since the Hill equation (2.5) is symmetric with respect to reflection $x \mapsto -x$ and admits only one linearly independent bounded eigenfunction $\psi = \psi_n(x)$ at $\omega = \omega_n$, the function $\psi_n(x)$ must be either even or odd in x. By the trace of the monodromy matrix [2], the periodic functions $\psi_n(x)$ correspond to the set $n \in S_+$ with $S_+ = \{0, 3, 4, 7, 8, \ldots\}$, and the antiperiodic functions $\psi_n(x)$ correspond to the set $n \in S_-$ with $S_- = \{1, 2, 5, 6, \ldots\}$. By Sturm's theorem [2], the periodic functions $\psi_n(x)$ with $n \in S_+$ have exactly $\text{ind}_{S_+}(n) - 1$ nodes on $x \in \left(-\frac{d}{2}, \frac{d}{2}\right)$, where $\text{ind}_{S_+}(n)$ is the order number of n in the set S_+. For instance, $\psi_0(x)$ has no nodes (positive definite), $\psi_3(x)$ has one node, $\psi_4(x)$ has two nodes, etc. Combining the symmetry with respect to reflections and the number of nodes, we conclude that the set of eigenfunctions $\{\psi_n(x)\}_{n \in S_+}$ alternates the symmetry in x, such that $\psi_0(x)$ is even, $\psi_3(x)$ is odd, $\psi_4(x)$ is even, etc. Similarly, the antiperiodic functions $\psi_n(x)$ with $n \in S_-$ have exactly $\text{ind}_{S_-}(n) - 1$ nodes on $x \in \left(-\frac{d}{2}, \frac{d}{2}\right)$. For instance, $\psi_1(x)$ has no nodes, $\psi_2(x)$ has one node, etc. We conclude again that the set of eigenfunctions $\{\psi_n(x)\}_{n \in S_-}$ alternates the symmetry in x, such that $\psi_1(x)$ is even, $\psi_2(x)$ is odd, etc.

Altogether, this set of facts is summarized in Table 1.

Table 1

Properties of the Bloch functions $\psi_n(x)$ and gap soliton bifurcations at the first eight band edges of an even potential $V_0(-x) = V_0(x)$.

n	0	1	2	3	4	5	6	7
symmetry	even	even	odd	odd	even	even	odd	odd
periodicity	S_+	S_-	S_-	S_+	S_+	S_-	S_-	S_+
# nodes on $\left(-\frac{d}{2}, \frac{d}{2}\right)$	0	0	1	1	2	2	3	3
sign of Γ_0 for local bifurcation	1	-1	1	-1	1	-1	1	-1

Let $\phi_0(x)$ be a single-humped solution of the ODE (2.3) with $\Gamma(x) = \Gamma_0$ and $V(x) = V_0(x)$ which bifurcates from the band edge $\omega = \omega_n$. By the local bifurcation theory [13], it inherits the symmetry properties (2.7) of the Bloch function $\psi_n(x)$. Therefore, $\phi_0(-x) = \phi_0(x)$ for branches of gap solitons to the left of ω_n with $n = \{0, 4, 8, \ldots\}$ (for $\Gamma_0 > 0$) and to the right

of ω_n with $n = \{1, 5, 9, \ldots\}$ (for $\Gamma_0 < 0$), while $\phi_0(-x) = -\phi_0(x)$ for branches of gap solitons to the left of ω_n with $n = \{2, 6, \ldots\}$ (for $\Gamma_0 > 0$) and to the right of ω_n with $n = \{3, 7, \ldots\}$ (for $\Gamma_0 < 0$). See Figures 2–3 in [13] for gap solitons $\phi_0(x)$ in the potential (2.6).

In this paper, we shall consider the existence of SGSs in the ODE (2.3) with piecewise constant coefficient $\Gamma(x) = \Gamma_\pm$ for $\pm x > 0$ and potential $V(x)$ of the following two classes:

$$\text{(2.8)} \qquad \text{(i) } V = V_0(x), \qquad \text{(ii) } V = V_0(x-\delta)\chi_{(-\infty,0)} + V_0(x+\delta)\chi_{[0,\infty)},$$

where $\chi_{[a,b]} = 1$ on $x \in [a, b]$ and zero otherwise, while $0 < \delta < d$. Here $V_0(x)$ is a smooth, even, d-periodic function on $x \in \mathbb{R}$. We note that $V(x)$ in (ii) is continuous and even on $x \in \mathbb{R}$ but smooth and periodic only on each $\pm x > 0$.

One can develop a general shooting method for numerical approximations of SGSs from the condition that a localized solution $\phi(x)$ of the second-order ODE (2.3) with $\omega \in (\omega_{2m-1}, \omega_{2m})$, $m \in \mathbb{N}$, decays to zero at infinity according to two fundamental solutions $p_\pm(x)e^{\mp\kappa x}$ as $x \to \pm\infty$, where $\kappa = \kappa(\omega)$ is a positive number. Solving the ODE (2.3) with $\Gamma(x) = \Gamma_+$ for a general initial value $\phi(0)$ and $\phi'(0)$ to $x > 0$ and the same ODE with $\Gamma(x) = \Gamma_-$ to $x < 0$, one can construct a continuously differentiable solution $\phi(x)$ on $x \in \mathbb{R}$ which decays to zero as $x \to \pm\infty$ if and only if the projections to the growing fundamental solutions $p_\pm(x)e^{\pm\kappa x}$ are zero at infinity. The system of two constraints for two initial values constitutes a well-posed problem of numerical analysis. This numerical approach was adopted in recent work [18]. Practical implementations of this algorithm are unclear as the shooting method may depend sensitively on starting approximations of the initial value and may require long computational time to search through all appropriate initial values. In addition, the ODE solvers of the shooting method may develop numerical instabilities in approximations of growing solutions.

Due to these reasons, we shall develop an alternative view on numerical approximations of SGSs, starting with local bifurcation analysis and using the homotopy continuation method to trace the solution families along parameters ω, $\Gamma_\pm$, and δ. Using these analytical and numerical results, we have obtained the following main results.

(1) We prove analytically that any gap soliton for $\Gamma_+ = \Gamma_-$ can be continued to the SGS for sufficiently small $|\Gamma_+ - \Gamma_-|$ under a nondegeneracy assumption.
(2) We prove analytically that the maximal difference $|\Gamma_+ - \Gamma_-|$ leading to SGS existence converges to 0 when ω approaches the band edge which features the local bifurcation of a gap soliton.
(3) SGSs are computed numerically when the potential $V(x)$ is given by (2.8)(i), and the maximal $|\Gamma_+ - \Gamma_-|$ allowing their existence is found. Our numerical results confirm the analytical results (1)–(2) above.
(4) Existence of SGSs for $V(x)$ in (2.8)(ii) with $\Gamma_+ > 0$ and $\Gamma_- < 0$ is studied. We numerically show that local bifurcations may occur from a countable set of points in the parameter domain $(\omega, \delta) \in (\omega_{2m-1}, \omega_{2m}) \times (0, d)$, $m \in \mathbb{N}$.
(5) We numerically compute the points of local bifurcation of SGSs for the potential (2.8)(ii) and use the homotopy continuation of the bifurcating solution. As a result, we show that the family of SGSs exists typically in a subset of the plane (ω, δ).
(6) We analytically show that the termination of families of SGSs for the potential (2.8)(ii) is related to existence of linear bound states for the nonsmooth potential.

Results (1)–(3) are reported in section 3, and results (4)–(6) are described in section 4.

3. Bifurcations of SGSs for smooth potentials. In this section we study continuation of SGSs from gap solitons existing for $\Gamma_+ = \Gamma_-$ in the case of a smooth potential function $V(x)$. A prototypical example of such potential is the symmetric function $V_0(x)$ in (2.8)(i).

3.1. Existence of bifurcations from gap solitons. Let $\gamma = (\Gamma_+ + \Gamma_-)/2$ and $\nu = (\Gamma_+ - \Gamma_-)/2$. Then, the ODE (2.3) can be rewritten in the form

$$F(\phi, \nu) = -\phi'' - \omega\phi + V(x)\phi - \gamma\phi^3 - \nu\,\mathrm{sign}(x)\phi^3 = 0, \tag{3.1}$$

where $F(\phi, \nu) : H^1(\mathbb{R}) \times \mathbb{R} \mapsto H^{-1}(\mathbb{R})$ is a nonlinear operator acting on a function $\phi(x)$ in space $H^1(\mathbb{R})$ and parameter $\nu \in \mathbb{R}$.

We assume that there exists a solution $\phi_0(x) \in H^1(\mathbb{R})$ for $\omega \in \mathbb{R} \setminus \Sigma$ and some γ and $V(x)$, such that $F(\phi_0, 0) = 0$. The Jacobian $D_\phi F(\phi_0, 0)$ is given by the Schrödinger operator $\mathcal{L} : H^2(\mathbb{R}) \mapsto L^2(\mathbb{R})$, where

$$\mathcal{L} = -\partial_x^2 - \omega + V(x) - 3\gamma\phi_0^2(x). \tag{3.2}$$

Since $\omega \in \mathbb{R}\setminus\Sigma$, we have $\phi_0^2(x) \to 0$ exponentially fast as $|x| \to \infty$, such that the term $-3\gamma\phi_0^2(x)$ is a relatively compact perturbation to the unbounded operator $L - \omega$, where $L = -\partial_x^2 + V(x)$. By a standard argument (see Corollary 2 in section XIII.4 in [14]), the essential spectrum of $\mathcal{L}$ and $(L - \omega)$ coincide. Since $\omega \in \mathbb{R} \setminus \Sigma$, the zero point is isolated from the essential spectrum of $\mathcal{L}$. If we further assume that $\mathcal{L}$ has the trivial kernel in $H^1(\mathbb{R})$, then $\mathcal{L}$ is invertible on $L^2(\mathbb{R})$. Since the translational invariance is broken if $V(x) \neq 0$, $\mathcal{L}$ generally has the trivial kernel, unless a bifurcation of branches of gap solitons occur. By the standard analysis based on the implicit function theorem, there exists a unique smooth continuation of $\phi_\nu(x)$ from $\phi_0(x)$ in $H^1(\mathbb{R})$ for sufficiently small ν, such that $F(\phi_\nu, \nu) = 0$ and $\phi_\nu(x) \to \phi_0(x)$ in $H^1(\mathbb{R})$ as $\nu \to 0$.

In other words, we have proved above that if a gap soliton exists for $\Gamma_+ = \Gamma_-$ and $\omega \in \mathbb{R} \setminus \Sigma$ and the linearized operator $\mathcal{L}$ is nondegenerate, then the gap soliton is uniquely continued into the SGS for small nonzero $|\Gamma_+ - \Gamma_-|$. We confirm this prediction via numerical analysis of the ODE (2.3) with $V(x)$ in (2.8)(i) for ω taken in the semi-infinite band gap and the first two finite gaps. Numerical approximations of $\phi_0(x)$ for $\Gamma_+ = \Gamma_-$ are obtained from the Newton–Raphson iterations and the homotopy continuation method. The initial guess for the Newton iteration is taken from an asymptotic expansion leading to the NLS approximation [13] when ω is close to the local bifurcation threshold ω_n. After a successful convergence for one such ω we use a standard homotopy continuation and generate a family of gap solitons $\phi_0(x)$ parameterized by ω. The discretization of the ODE (2.3) is based on a fourth-order central difference approximation of ∂_{xx} on a truncated domain with zero Dirichlet boundary conditions.

3.2. Numerical computations of SGSs. We now proceed to construct SGSs, i.e., solutions $\phi(x)$ of the second-order ODE (2.3) with $\Gamma_+ \neq \Gamma_-$. When $\phi_0(x)$ is obtained for a given value of ω, we can apply the numerical homotopy continuation of the solution by deviating Γ_- from Γ_+. At each step, the SGS $\phi(x)$ is thus found via Newton's iterations. The final value of Γ_-, up to which the iteration converges, is denoted by Γ_*.

Figure 1 shows the values of Γ_* for $\Gamma_+ = +1$ (a) and $\Gamma_+ = -1$ (b). The computational tolerance in Γ_* is 0.006 inside the band gaps and 0.002 near the band edges. In the case

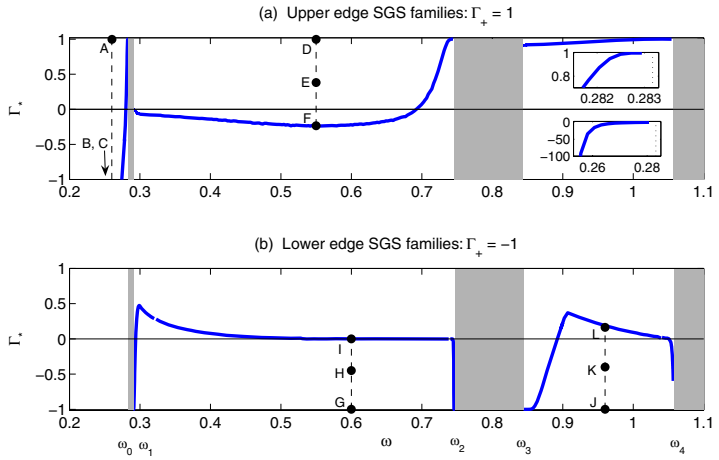

Figure 1. *The values of Γ_* for SGSs originating from symmetric GS families of the first three frequency gaps of $V(x) = \sin^2(\pi x/10)$. In* (a) *the upper inset zooms in and the lower inset zooms out on the graph in the semi-infinite gap. The points A–L are referenced in Figure 2.*

$\Gamma_+ = 1$, local bifurcations of small-amplitude gap solitons occur from the lower band edges. Figure 1(a) shows that the SGSs exist in the semi-infinite gap, as well as in the first two frequency gaps. In the case $\Gamma_+ = -1$, local bifurcations of gap solitons occur from the upper band edges. Figure 1(b) shows that the SGSs exist in the first and second frequency gaps. The two insets of Figure 1(a) show that Γ_* decreases quickly as ω moves away from the edge of the first band and that the convergence $\Gamma_* \uparrow 1$ as $\omega \uparrow \omega_0$ is smooth. We further see from Figure 1 that the interval of existence shrinks as ω approaches the value ω_n for any band edge, where gap solitons undertake a local bifurcation. In addition, the interval of existence is extremely large in the semi-infinite gap $(-\infty, \omega_0)$, but it becomes narrow in the finite gaps $(\omega_{2m-1}, \omega_{2m})$ for $m \geq 1$.

For comparison, the family of SGSs in the gap (ω_1, ω_2) exists for $-0.24 < \Gamma_* < 1$ in the case $\Gamma_+ = +1$ and $-1 < \Gamma_* < 0.47$ in the case $\Gamma_+ = -1$. The family of SGSs in the gap (ω_3, ω_4) exists in a very narrow region of $0.92 < \Gamma_* < 1$ in the case $\Gamma_+ = +1$ and in a bigger interval $-1 < \Gamma_* < 0.37$ in the case $\Gamma_+ = -1$ (similarly to that in the first gap).

Figure 2 shows profiles of SGSs which correspond to the twelve points labeled A–L in Figure 1. The solid lines correspond to the gap solitons from which the homotopy in Γ_- is started (i.e., points A, D, G, and J). Clearly, the total power and maximum amplitude of the SGSs increase as $|\Gamma_+ - \Gamma_-|$ increases. Also notice that the profiles become more concentrated on the half $x > 0$ in the case $\Gamma_+ = +1$ (see Figure 2 (a–b)) and on the half $x < 0$ in the case $\Gamma_+ = -1$ (see Figure 2 (c–d)) as $|\Gamma_+ - \Gamma_-|$ increases. This is in accord with the law of refraction: when $\Gamma_+ = +1$ and Γ_- decreases from 1, the half $x > 0$ becomes relatively more focusing and therefore attracts more energy of the soliton, while when $\Gamma_+ = -1$ and Γ_- increases from -1, the situation is the opposite.

3.3. Asymptotic analysis near gap soliton bifurcation points. Now we shall explain why the existence interval shrinks to zero when ω approaches the value ω_n where a local bifurcation

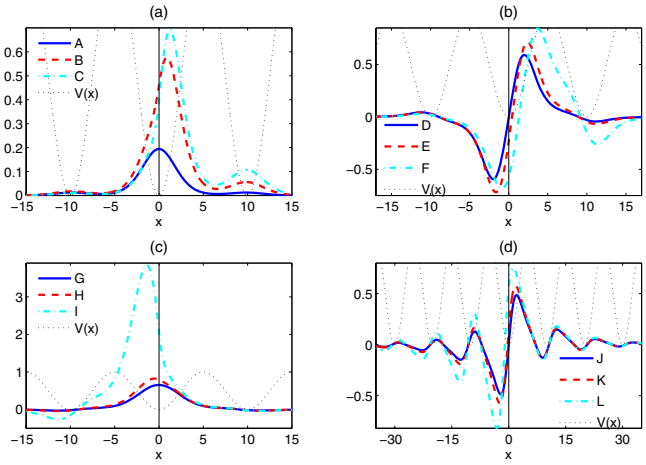

Figure 2. *The profiles of SGSs corresponding to the points A–L in Figure 1. Values of ω are A–C:* 0.26, *D–F:* 0.55, *G–I:* 0.6, *J–L:* 0.96. *Values of Γ_- are A:* 1, *B:* -3.9, *C:* -15.3, *D:* 1, *E:* 0.38, *F:* -0.235, *G:* -1, *H:* -0.45, *I:* 0.002, *J:* -1, *K:* -0.4, *L:* 0.164.

of gap solitons occurs. As $\omega \to \omega_n$, we have $\|\phi_0\|_{L^\infty} \to 0$ and $\mathcal{L} \to (L-\omega_n)$. Since the operator $(L-\omega_n)$ is not invertible, the implicit function theorem cannot be used and the solution $\phi_0(x)$ cannot be continued beyond $\nu = 0$. In order to give a more precise explanation of this phenomenon, we adopt the NLS approximation for local bifurcation of gap solitons from [13] (see also the review in [12]). In particular, we consider an asymptotic solution to the ODE (2.3),

$$\begin{aligned} &\omega = \omega_n + \varepsilon^2\,\Omega + \mathcal{O}(\varepsilon^4), \\ &\phi(x) = \varepsilon\,A(X)\psi_n(x) + \varepsilon^2\,A'(X)\tilde{\psi}_n(x) + \varepsilon^3\,\phi^{(3)}(x,X) + \mathcal{O}(\varepsilon^4), \end{aligned} \tag{3.3}$$

where $X = \varepsilon\,x$, $\varepsilon << 1$, the function $A(X)$ and parameter Ω are defined below, and ψ_n and $\tilde{\psi}_n$ are the d-periodic (or d-antiperiodic) Bloch functions and generalized Bloch functions, respectively, of the Hill equation (2.5) for $\omega = \omega_n$, such that

$$(L-\omega_n)\psi_n = 0, \qquad (L-\omega_n)\tilde{\psi}_n = 2\psi_n'. \tag{3.4}$$

The correction term $\phi^{(3)}(x,X)$ at $\mathcal{O}(\varepsilon^3)$ solves the nonhomogeneous problem

$$(L-\omega_n)\phi^{(3)} = \Omega A\psi_n + A''\psi_n + 2A''\tilde{\psi}_n' + \Gamma(X)A^3\psi_n^3. \tag{3.5}$$

To ensure boundedness of $\phi^{(3)}(x,X)$ with respect to the variable x, and, hence, legitimacy of the expansion (3.3), one has to apply the Fredholm alternative which imposes the orthogonality condition of the right-hand side of (3.5) with respect to $\psi_n(x)$ on $x \in [0,d]$. The orthogonality condition is written as

$$\Omega A + \mu A'' + \rho\Gamma(X)A^3 = 0, \tag{3.6}$$

where

$$\mu = 1 + 2\frac{(\tilde{\psi}_n', \psi_n)}{(\psi_n, \psi_n)}, \qquad \rho = \frac{(\psi_n^2, \psi_n^2)}{(\psi_n, \psi_n)},$$

and we have used the standard L^2 inner product $(\cdot, \cdot)$ over one period $x \in [0, d]$. It is shown in [13] that $\mu = \frac{1}{2}\omega''_{2n,2n+1}(k)$ with either $k = 0$ or $k = \frac{\pi}{d}$ at the point $\omega = \omega_n$, where $\omega_{2n,2n+1}(k)$ is the dispersion relation between $\omega \in [\omega_{2n}, \omega_{2n+1}]$ and $k \in [0, \frac{\pi}{d}]$.

Due to the nature of the nonlinearity interface, the function $\Gamma(X)$ is the same as $\Gamma(x)$, i.e., $\Gamma(X) = \Gamma_\pm$ for $\pm X > 0$. We shall prove that no localized solution of the ODE (3.6) exists under the condition $\Gamma_- \neq \Gamma_+$. Indeed, consider the Hamiltonian of the ODE (3.6):

$$H[A] = \frac{1}{2}\left[\mu (A')^2 + \Omega A^2\right] + \frac{1}{4}\rho\Gamma(X)A^4. \tag{3.7}$$

If $A(X)$ solves the ODE (3.6), then

$$\frac{d}{dX}H[A(X)] = \frac{1}{4}\rho\Gamma'(X)A^4(X) = \frac{1}{4}\rho(\Gamma_+ - \Gamma_-)\delta(X)A^4(X),$$

where $\delta(X)$ is the Dirac delta-function. If $A(X)$ is a localized solution on $X \in \mathbb{R}$, then the integration on $X \in \mathbb{R}$ gives the constraint

$$0 = \lim_{x\to+\infty} H[A(X)] - \lim_{x\to-\infty} H[A(X)] = \frac{1}{4}\rho(\Gamma_+ - \Gamma_-)A^4(0),$$

since $H[A(X)] \to 0$ if $A(X), A'(X) \to 0$ as $|X| \to \infty$. Therefore, $A(0) = 0$ if $\Gamma_+ \neq \Gamma_-$. Consider now $H[A(X)]$ on $X > 0$. It is clear from the decaying conditions as $X \to \infty$ that $H[A(X)] = \text{const} = 0$, which together with the fact that $A(0) = 0$ leads to $0 = \lim_{X\downarrow 0} H[A(X)] = \frac{1}{2}\mu|A'(0)|^2$, such that $A'(0) = 0$. The only solution of the ODE (3.6) with $A(0) = A'(0) = 0$ is the zero solution $A(X) \equiv 0$.

If $\Gamma_+ = \Gamma_- = \Gamma_0$ and $\text{sign}(\mu) = \text{sign}(\rho\Gamma_0) = -\text{sign}(\Omega)$, the ODE (3.6) has the standard sech-soliton decaying as $|X| \to \infty$. However, the result above shows that the sech-soliton with $\Gamma_+ = \Gamma_-$ cannot be homotopically continued to a decaying solution of (3.6) for $\Gamma_+ \neq \Gamma_-$. This proves that $\Gamma_* \to \Gamma_+$ as $\omega \to \omega_n$, where ω_n is a local bifurcation value.

4. Bifurcations of SGSs for nonsmooth potentials.

In this section, we study local bifurcations of solutions of the ODE (2.3) when $V(x)$ is a continuous function with the jump in the first derivative at the nonlinearity interface. The prototypical example of such potentials is given by (2.8)(ii), where $V_0(x)$ is an even potential (in our numerical computations we use V_0 from (2.6)). We shall consider the existence of SGSs under the normalization $\Gamma_+ = -\Gamma_- = +1$.

4.1. SGS numerical construction via gluing.

The point (δ_*, ω_*) in the parameter domain $\delta \in (0, d)$ and $\omega \in (\omega_{2m-1}, \omega_{2m})$, $m \in \mathbb{N}$, is defined to be a point of a local bifurcation of SGSs according to the following two-step algorithm.

(i) *Construction of continuous solutions.* Let $\phi_\pm(x; \omega)$ denote the family of single-humped gap solitons parameterized by $\omega \in (\omega_{2m-1}, \omega_{2m})$ and centered at $x = 0$ corresponding to (2.3) with $\Gamma(x) \equiv \Gamma_\pm$, respectively. These families bifurcate from the points $\omega = \omega_{2m}$ for $\Gamma_+ > 0$

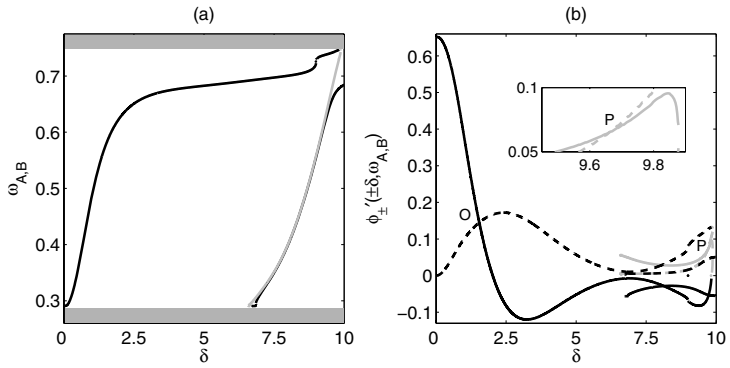

Figure 3. *Two-step search for (ω_*, δ_*) in the gap (ω_1, ω_2). (a) Result of step* (i)*—parametrization of the families of continuous solutions (4.1): black line $\omega_A(\delta)$, gray line $\omega_B(\delta)$. (b) Step* (ii)*—search for δ_*: solid black $\phi_+'(\delta;\omega_A)$, dashed black $\phi_-'(-\delta;\omega_A)$, solid gray $-\phi_+'(\delta;\omega_B)$, and dashed gray $\phi_-'(-\delta;\omega_B)$. Labeled points correspond to SGSs.*

and $\omega = \omega_{2m-1}$ for $\Gamma_- < 0$. In order to find continuous solutions, we now study for each fixed $\delta \in (0, d)$ the two functions

$$f_A(\omega) = \phi_-(-\delta;\omega) - \phi_+(\delta;\omega), \quad f_B(\omega) = \phi_-(-\delta;\omega) + \phi_+(\delta;\omega)$$

and find their zeros denoted by $\omega_{A,B} = \omega_{A,B}(\delta)$, respectively. For each δ existence of zeros of either $f_A(\omega)$ or $f_B(\omega)$ is guaranteed by continuity of $\phi_\pm$ as functions of ω and by the fact that $\phi_-(-\delta;\omega_{2m-1}) = \phi_+(\delta;\omega_{2m}) = 0$ and $\phi_-(-\delta;\omega_{2m}) \neq 0$, $\phi_+(\delta;\omega_{2m-1}) \neq 0$. Moreover, several zeros of these functions may occur for the same δ.

When a zero $\omega_A(\delta)$ or $\omega_B(\delta)$ is found, a δ-parameterized family of continuous solutions $\phi_A(x;\delta)$ or $\phi_B(x;\delta)$, respectively, is constructed by gluing two individual gap solitons:

$$\begin{aligned} \phi_A(x;\delta) &= \phi_-(x-\delta;\omega_A)\chi_{(-\infty,0)} + \phi_+(x+\delta;\omega_A)\chi_{[0,\infty)}, \\ \phi_B(x;\delta) &= \phi_-(x-\delta;\omega_B)\chi_{(-\infty,0)} - \phi_+(x+\delta;\omega_B)\chi_{[0,\infty)}. \end{aligned} \tag{4.1}$$

The functions $\phi_{A,B}(x;\delta)$ decay as $|x| \to \infty$ and are smooth in x everywhere except at the nonlinearity interface $x = 0$, where they generally have a jump in the first derivative.

Note that it is important to consider both ϕ_A and ϕ_B due to the sign invariance of the ODE (2.3). Each sign produces a branch of continuous solutions of the ODE (2.3).

Figures 3 (a) and 4 (a) present the numerically computed $\omega_{A,B}(\delta)$ for $\delta \in (0, d)$ in the gaps (ω_1, ω_2) and (ω_3, ω_4), respectively. The lack of smoothness in the curves in these figures is due to an insufficient resolution in the search algorithm and can be corrected with a finer resolution. Note that when $\omega_{A,B}(\delta)$ is multiple-valued, as seen in Figures 3 (a) and 4 (a), we may have several decaying solutions $\phi_A(x)$ and/or $\phi_B(x)$ for the same δ.

(ii) *Construction of SGSs.* Next, we search for continuously differentiable solutions within the above family $\phi_{A,B}(x;\delta)$. To ensure the continuity of the first derivative of $\phi(x;\delta)$ at $x = 0$, we search for zeros of the two functions

$$g_A(\delta) = \phi_-'(-\delta;\omega_A) - \phi_+'(\delta;\omega_A), \quad g_B(\delta) = \phi_-'(-\delta;\omega_B) + \phi_+'(\delta;\omega_B).$$

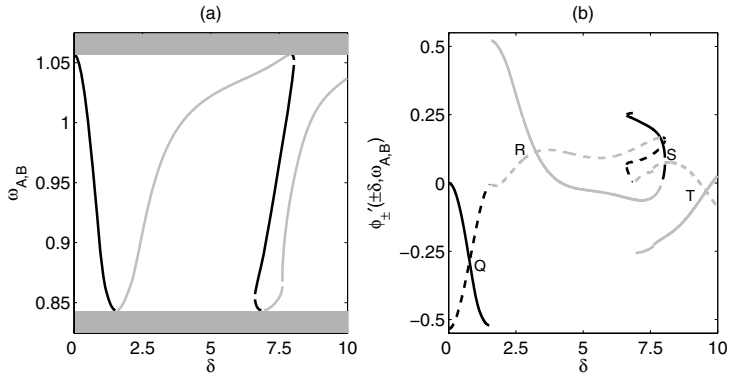

Figure 4. *Analogous to Figure 3 but for the gap* (ω_3, ω_4).

If a zero of either $g_A(\delta)$ or $g_B(\delta)$, denoted by δ_*, exists, then the function $\phi_A(x;\delta_*)$ or $\phi_B(x;\delta_*)$, respectively, in (4.1) has a continuous first derivative across the point $x = 0$. Figures 3 (b) and 4 (b) present the numerical results on computing δ_*. The labeled intersection points O, P, Q, R, S, and T correspond to zeros of $g_{A,B}(\delta)$. They are found as intersection points of solid and dashed curves of the same color. The solid black line shows the plot of $\phi'_+(\delta;\omega_A)$, and the dashed black line shows $\phi'_-(-\delta;\omega_A)$. Similarly, the solid gray line plots $-\phi'_+(\delta;\omega_B)$, and the dashed gray line plots $\phi'_-(-\delta;\omega_B)$. Therefore, an intersection of a solid black and a dashed black line (points O, Q, S) gives zeros δ_* of $g_A(\delta)$ and, thus, a solution $\phi_A(x;\delta_*)$. Similarly, an intersection of a solid gray and a dashed gray line (points P, R, T) gives zeros δ_* of $g_B(\delta)$ and, thus, a solution $\phi_B(x;\delta_*)$.

Table 2 shows the approximate computed values of δ_* and corresponding $\omega_* = \omega_{A,B}(\delta_*)$ at the points O–T for branches A, B of solutions given by (4.1). Note that additional points (δ_*, ω_*) can be obtained by generalizing the above functions $f_{A,B}$ and $g_{A,B}$ to

$$f_{j_A}(\omega) = \phi_-(-(jd+\delta);\omega) - \phi_+(jd+\delta;\omega), \quad f_{j_B}(\omega) = \phi_-(-(jd+\delta);\omega) + \phi_+(jd+\delta;\omega)$$

and

$$g_{j_A}(\delta) = \phi'_-(-(jd+\delta);\omega_A) - \phi'_+(jd+\delta;\omega_A), \quad g_{j_B}(\delta) = \phi'_-(-(jd+\delta);\omega_B) + \phi'_+(jd+\delta;\omega_B)$$

for $j \in \{1, 2, \ldots\}$ with V still defined as in (2.8)(ii). Nontrivial points (ω_*, δ_*) may exist for any such j. For example, we have found one such point for $j = 1$. The computed value is $(\omega_*, \delta_*) \approx (0.73, 7.33)$, and the resulting SGS corresponds to the point Z in Figure 5(a). Such additional solutions are SGSs of smaller amplitude compared to those for $j = 0$.

Table 2

Bifurcation points for SGSs in the domain $\omega \in (\omega_1, \omega_2) \cup (\omega_3, \omega_4)$ *and* $\delta \in (0, d)$.

Point	O	P	Q	R	S	T
Branch of solution	A	B	A	B	A	B
ω_*	0.58	0.70	0.94	0.97	1.03	1.03
δ_*	1.54	9.66	0.78	3.24	7.97	9.57

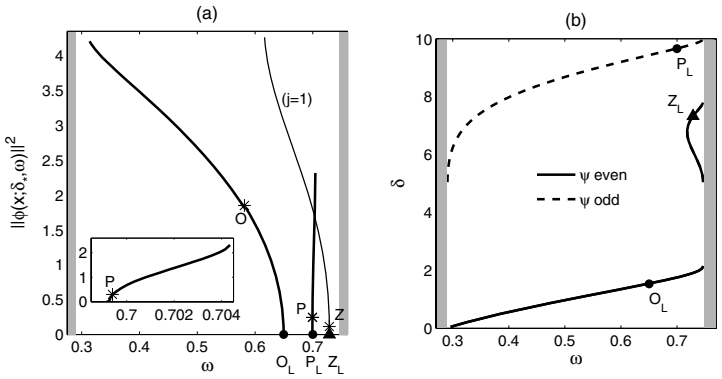

Figure 5. (a) *SGS continuation curves, total power versus frequency, in the gap* (ω_1, ω_2). *Labeled points* O, P *correspond to those in Figure* 3 (b). *Point* Z *is discussed in section* 4.1. *Points* O_L, P_L, *and* Z_L *are SGS termination points.* (b) *Point spectrum of the linear Schrödinger operator inside* (ω_1, ω_2) *for all* $\delta \in (0, d)$. *Solid/dashed lines: eigenvalues with even/odd eigenfunctions.*

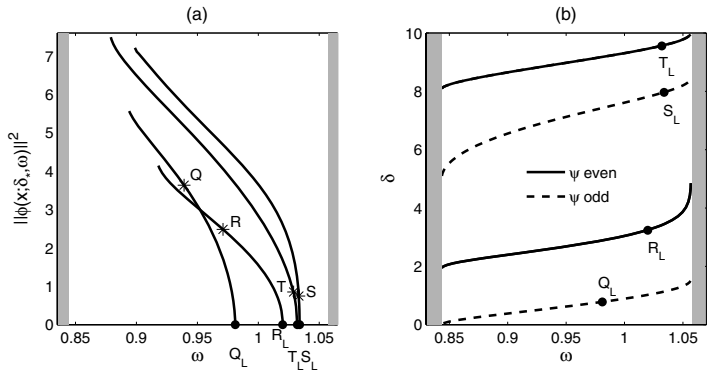

Figure 6. (a) *SGS continuation curves, total power versus frequency, in the gap* (ω_3, ω_4). *Labeled points* Q–T *correspond to those in Figure* 4 (b). *Points* Q_L–T_L *are SGS termination points.* (b) *Point spectrum of the linear Schrödinger operator inside* (ω_3, ω_4) *for all* $\delta \in (0, d)$. *Solid/dashed lines: eigenvalues with even/odd eigenfunctions.*

4.2. Numerical homotopy continuation of SGSs. Assuming the existence of a point (ω_*, δ_*), we have constructed the SGS of the ODE (2.3), where the potential function $V(x)$ is given by (2.8)(ii) and $(\omega, \delta) = (\omega_*, \delta_*)$. The SGS denoted as $\phi_*(x)$ is represented by one of the functions in (4.1) with $(\omega, \delta) = (\omega_*, \delta_*)$. Each of these solutions can be used as a starting point for a numerical homotopy continuation to generate a family of SGSs parameterized by $\omega \subset (\omega_{2m-1}, \omega_{2m})$ for a given value of $\delta = \delta_*$. Similarly, for a fixed $\omega = \omega_*$ a family parameterized by $\delta \subset (0, d)$ can be constructed. Under the same assumption that the operator $\mathcal{L} = -\partial_x^2 - \omega_* + V(x) - 3\Gamma(x)\phi_*^2(x)$ is invertible, the implicit function theorem implies that there exists a unique smooth continuation of the particular solution $\phi_*(x)$ to the family of solutions along parameters ω and δ.

We restrict our numerical studies to the continuation in ω. Numerical results of such continuation from the SGSs at points O–T are shown in Figures 5 (a) and 6 (a). The curves

plot the total soliton power $\|\phi\|^2_{L^2(\mathbb{R})}$ as a function of frequency ω for fixed $\delta = \delta_*$. Note that each curve corresponds to a different value of δ_* and hence a different potential $V(x)$. The values of δ_* can be read in Table 2. Termination of a continuation curve is defined when the total power of the soliton becomes zero or when Newton iteration convergence fails. As the figures show, the latter case is always accompanied by the slope of the continuation curve becoming infinite, suggesting a violation of the implicit function theorem assumptions. The former termination case is studied in the following subsection.

4.3. Analysis of termination points of SGSs. We shall now consider the termination points of the solution families plotted in Figures 5 (a) and 6 (a), where the soliton power becomes zero. The points are labeled O_L–T_L, and their corresponding values of δ and ω are given in Table 3.

Table 3
Termination points for the six SGS families in Figures 5 (a) and 6 (a).

Point	O_L	P_L	Q_L	R_L	S_L	T_L
δ	1.54	9.66	0.78	3.24	7.97	9.57
ω	0.65	0.70	0.98	1.02	1.03	1.03

The termination points are expected to be related to the existence of nontrivial bound states in the (point) spectrum of the Schrödinger operator for the same potential $V(x)$, i.e., with exponentially decaying solutions of the linear ODE

$$-\psi'' - \omega\psi + V(x)\psi = 0, \qquad \psi : \mathbb{R} \mapsto \mathbb{R}, \tag{4.2}$$

for $V(x)$ in (2.8)(ii) and $\omega \in \mathbb{R}\backslash\Sigma$. The point spectrum is nonempty due to the singularity of $V(x)$ at $x = 0$.

4.3.1. Numerical results. Results of numerical computations of the point spectrum contained in the first two finite gaps (ω_1, ω_2) and (ω_3, ω_4) are shown in Figures 5 (b) and 6 (b) for all values $\delta \in [0, d]$. The eigenfunctions ψ are either even (solid lines) or odd (dashed lines). For the six values of δ corresponding to the SGS families in Figures 5 (a) and 6 (a) the eigenvalues are marked by black dots and are in perfect agreement with the values of ω at the termination points O_L–T_L. The symmetry (even/odd) of the bound states at O_L–T_L also matches that of the eigenfunctions at the marked points in the point spectrum. The eigenvalue curve originating as well as ending at ω_2 in Figure 5 (b) corresponds to the termination point Z_L of the SGS family for $j = 1$ in Figure 5 (a). The termination point Z_L for the same value of δ is shown by a triangle.

4.3.2. Bifurcation analysis for $|\delta|$ small. In this subsection we consider bifurcations of point spectrum of the Schrödinger operator from the band edges for small values of $|\delta|$ (or, due to the d periodicity of V, equivalently for δ near 0 from above and near d from below). This analysis will prove the existence of the spectral curves near $\delta = 0$ and $\delta = 10$ in Figures 5 (b) and 6 (b), i.e., the existence of curves with points O_L and Q_L locally to $\delta = 0$ and the curves with points P_L and T_L locally to $\delta = 10$.

In order to construct solutions of the spectral problem (4.2), we first consider exponentially decaying solutions of the ODE on the half-line

$$-\psi_+'' - \omega\psi_+ + V_0(x+\delta)\psi_+ = 0, \qquad \psi_+ : \mathbb{R}_+ \mapsto \mathbb{R}.$$

By using the fundamental solution of the Hill equation (2.5), we can express $\psi_+(x)$ in the form $\psi_+ = e^{-\kappa x}u_-(x+\delta)$, where $u_-(x)$ are periodic or antiperiodic bounded solutions of the Hill equation (2.5) with $V(x) = V_0(x)$.

As $V(x)$ is even, the function $\psi_+(x)$ admits a symmetric (even) reflection about $x = 0$ if $\psi_+'(0) = 0$, which is equivalent to the condition

$$G_1(\delta,\kappa) = u_-'(\delta) - \kappa u_-(\delta) = 0,$$

and it admits an antisymmetric (odd) reflection about $x = 0$ if $\psi_+(0) = 0$, which is equivalent to the condition

$$G_2(\delta,\kappa) = u_-(\delta) = 0.$$

Since eigenvalues of the spectral problem (4.2) are simple and the eigenfunctions are either even or odd, all eigenvalues of the spectral problem (4.2) in the band gaps $\omega \in \mathbb{R}\backslash\Sigma$ are defined by zeros of the functions $G_1(\delta,\kappa)$ and $G_2(\delta,\kappa)$ in κ for a given value of δ, where $\kappa \geq 0$ and the values of κ are related to the values of ω in the band gaps. Both functions $G_{1,2}$ are analytic in $\delta \in \mathbb{R}$ and periodic with period d. Both functions admit analytic continuation in the parameter $\kappa \in \mathbb{R}_+$ [8].

If $\delta = 0$, the only zeros of $G_1(\delta,\kappa)$ and $G_2(\delta,\kappa)$ occur at $\kappa = 0$, i.e., at the band edges $\omega = \omega_n$. Indeed, if $G_1(0,\kappa) = 0$, then $\psi_+'(0) = 0$, such that $\psi_+(x) = \psi_n(x)$ is an even function on $x \in \mathbb{R}$. However, $\psi_+(x)$ decays exponentially as $x \to \infty$ and grows exponentially as $x \to -\infty$ if $\kappa > 0$. Therefore, $G_1(0,\kappa) = 0$ is equivalent to $\kappa = 0$. A similar argument works for $G_2(0,\kappa) = 0$.

(i) *Bifurcation of even eigenfunctions.* Let us first consider the zeros of $G_1(\delta,\kappa)$. Computing the derivatives of $G_1(\delta,\kappa)$ in δ and κ at $(\delta,\kappa) = (0,0)$, we obtain

$$\partial_\delta G_1(0,0) = u_-''(0) = \psi_n''(0) = (V_0(0) - \omega_n)\psi_n(0),$$
$$\partial_\kappa G_1(0,0) = -\tilde{\psi}_n'(0) - \psi_n(0),$$

where $\tilde{\psi}_n$ is the generalized Bloch function; see (3.4). The fact that $\tilde{\psi}_n = -\frac{\partial u_-}{\partial\kappa}\big|_{\kappa=0}$ is clear from differentiation of (2.5) with respect to κ.

It is found in [12] that

$$D(x) = \psi_n(x)\tilde{\psi}_n'(x) - \psi_n'(x)\tilde{\psi}_n(x) + \psi_n^2(x)$$

is constant in x, i.e., $D(x) = D(0)$, and that

$$D(0) = \frac{1}{2}\omega_{2n-1,2n}''(k)(\psi_n,\psi_n), \tag{4.3}$$

where either $k = 0$ or $k = \frac{\pi}{d}$ at the bifurcation point $\omega = \omega_n$. Since $\psi_n'(0) = 0$, $D(0) = \psi_n(0)(\tilde{\psi}_n'(0)+\psi_n(0))$, and the leading-order approximation for the root of $G_1(\delta,\kappa)$ near $(\delta,\kappa) =$

$(0,0)$ is given by

$$\delta = \frac{\tilde{\psi}_n'(0) + \psi_n(0)}{\psi_n(0)(V_0(0) - \omega_n)}\kappa + \mathcal{O}(\kappa^2) = \frac{D(0)}{\psi_n^2(0)(V_0(0) - \omega_n)}\kappa + \mathcal{O}(\kappa^2),$$

where $\psi_n(0) \neq 0$ (which is met since $\psi_n'(0) = 0$). Using (4.3) and the facts that $\omega_n > 0$ and $V_0(0) = 0$ for the numerical example (2.6), we get

$$\delta = -\frac{\omega_{2n-1,2n}''(k)(\psi_n, \psi_n)}{2\psi_n^2(0)\omega_n}\kappa + \mathcal{O}(\kappa^2).$$

Therefore, the bifurcation occurs for $\delta > 0$ if $\omega_{2n-1,2n}''(k) < 0$ (e.g., for ω to the right of ω_1) and for $\delta < 0$ if $\omega_{2n-1,2n}''(k) > 0$ (e.g., for ω to the left of ω_0 and ω_4); see Table 1. Note that the negative values of δ correspond to the values of δ below the level $\delta = d$ due to periodicity of the function $G_1(\delta, \kappa)$ in δ. The above local existence analysis for even bound states is confirmed by the solid lines near $\delta = 0$ in Figure 5 (b) and near $\delta = d = 10$ in Figure 6 (b).

(ii) *Bifurcation of odd eigenfunctions.* Similarly to (i), we study the zeros of $G_2(\delta, \kappa)$. We compute the derivatives of $G_2(\delta, \kappa)$ in δ and κ at $(\delta, \kappa) = (0, 0)$,

$$\partial_\delta G_2(0,0) = u_-'(0) = \psi_n'(0),$$
$$\partial_\kappa G_2(0,0) = -\tilde{\psi}_n(0),$$

such that the leading-order approximation for the root of $G_2(\delta, \kappa)$ near $(\delta, \kappa) = (0, 0)$ is given by

$$\delta = \frac{\tilde{\psi}_n(0)}{\psi_n'(0)}\kappa + \mathcal{O}(\kappa^2) = -\frac{\omega_{2n-1,2n}''(k)(\psi_n, \psi_n)}{2(\psi_n'(0))^2}\kappa + \mathcal{O}(\kappa^2),$$

where $\psi_n'(0) \neq 0$ (which is met since $\psi_n(0) = 0$). From the expansion, we conclude that the bifurcation occurs for $\delta > 0$ if $\omega_{2n-1,2n}''(k) < 0$ (e.g., for ω to the right of ω_3) and for $\delta < 0$ if $\omega_{2n-1,2n}''(k) > 0$ (e.g., for ω to the left of ω_2). The dashed lines near $\delta = 0$ in Figure 6 (b) and near $\delta = d = 10$ in Figure 5 (b) confirm this analysis.

Note that there are curves in Figures 5 (b) and 6 (b) which do not bifurcate from $\delta = 0$ and $\delta = d = 10$ but still bifurcate from the band edge $\omega = \omega_n$. Bifurcations of these curves cannot be confirmed from the analytical theory above, unless the values of $G_{1,2}(\delta; 0)$ for $0 < \delta < d$ are approximated numerically.

5. Conclusion.

We have employed methods of bifurcation theory for the existence problem of SGSs supported by the nonlinearity interface and the periodic potential. Two bifurcation problems are considered numerically. The first bifurcation takes place from the standard gap solitons existing at the zero jump of the nonlinearity coefficient. The second bifurcation takes place from the bound state consisting of parts of two standard gap solitons glued together in a continuously differentiable SGS. Three asymptotic results are described in the article. We show that the standard gap solitons can be continued generally for small jumps in the nonlinearity coefficient. On the contrary, no SGSs for nonzero jump of the nonlinearity coefficient exist in the NLS approximation which is valid near the band edges. In addition, we analytically study bifurcations of eigenvalues of the Schrödinger operator with a nonsmooth potential from band edges of the Hill equation.

One can argue that the SGSs bifurcating from a standard gap soliton or a gluing combination of two gap solitons inherit stability properties of gap solitons in the neighborhood of the local bifurcation points. Stability of standard gap solitons was considered analytically and numerically in [13]. The stability properties can change far from the bifurcation points. Detailed computations of stability of the SGSs will be the subject of a forthcoming work.

Acknowledgment. Dmitry Pelinovsky thanks the people at ETH Zürich for hospitality during his visit.

REFERENCES

[1] D. Blömer, A. Szameit, F. Dreisow, T. Schreiber, S. Nolte, and A. Tünnermann, *Nonlinear refractive index of fs-laser-written waveguides in fused silica*, Opt. Express, 14 (2006), pp. 2151–2157.
[2] M. S. Eastham, *The Spectral Theory of Periodic Differential Equations*, Scottish Academic Press, Edinburgh, 1973.
[3] G. Fibich, Y. Sivan, and M. I. Weinstein, *Bound states of nonlinear Schrödinger equations with a periodic nonlinear microstructure*, Phys. D, 217 (2006), pp. 31–57.
[4] J. Hudock, S. Suntsov, D. Christodoulides, and G. Stegeman, *Vector discrete nonlinear surface waves*, Opt. Express, 13 (2005), pp. 7720–7725.
[5] Y. V. Kartashov, A. A. Egorov, V. A. Vysloukh, and L. Torner, *Surface vortex solitons*, Opt. Express, 14 (2006), pp. 4049–4057.
[6] Y. V. Kartashov and L. Torner, *Multipole-mode surface solitons*, Opt. Lett., 31 (2006), pp. 2172–2174.
[7] Y. V. Kartashov, V. A. Vysloukh, and L. Torner, *Surface gap solitons*, Phys. Rev. Lett., 96 (2006), 073901.
[8] W. Kohn, *Analytic properties of Bloch waves and Wannier functions*, Phys. Rev. (2), 115 (1959), pp. 809–821.
[9] W. Magnus and S. Winkler, *Hill's Equation*, Interscience Tracts in Pure and Applied Mathematics 20, John Wiley & Sons, New York, London, Sydney, 1966.
[10] K. G. Makris, S. Suntsov, D. N. Christodoulides, G. I. Stegeman, and A. Hache, *Discrete surface solitons*, Opt. Lett., 30 (2005), pp. 2466–2468.
[11] A. Pankov, *Periodic nonlinear Schrödinger equation with application to photonic crystals*, Milan J. Math., 73 (2005), pp. 259–287.
[12] D. Pelinovsky, *Asymptotic reductions of the Gross–Pitaevskii equation*, in Emergent Nonlinear Phenomena in Bose–Einstein Condensates: Theory and Experiment, P. Kevrekidis, D. Frantzeskakis, and R. Carretero, eds., Springer-Verlag, Heidelberg, 2007, pp. 377–398.
[13] D. E. Pelinovsky, A. A. Sukhorukov, and Y. Kivshar, *Bifurcations and stability of gap solitons in periodic structures*, Phys. Rev. E (3), 70 (2004), 036618.
[14] B. Simon and M. Reed, *Methods of Modern Mathematical Physics* IV: *Analysis of Operators*, Academic Press, New York, 1978.
[15] Y. Sivan, G. Fibich, and M. I. Weinstein, *Waves in nonlinear lattices—ultrashort optical pulses and Bose–Einstein condensates*, Phys. Rev. Lett., 97 (2006), 193902.
[16] S. Suntsov, K. G. Makris, D. N. Christodoulides, G. I. Stegeman, A. Hache, R. Morandotti, H. Yang, G. Salamo, and M. Sorel, *Observation of discrete surface solitons*, Phys. Rev. Lett., 96 (2006), 063901.
[17] W. J. Tomlinson, *Surface wave at a nonlinear interface*, Opt. Lett., 5 (1980), pp. 323–325.
[18] D. A. Zezyulin, G. L. Alfimov, V. V. Konotop, and V. M. Perez-Garcia, *Control of nonlinear modes by scattering-length management in Bose–Einstein condensates*, Phys. Rev. A (3), 76 (2007), 013621.